Chem Soc Rev

RSC Publishing

TUTORIAL REVIEW

View Article Online
View Journal | View Issue

Cite this: *Chem. Soc. Rev.*, 2013, **42**, 6019

Recent progress in luminescent and colorimetric chemosensors for detection of thiols

Hyo Sung Jung,[a] Xiaoqiang Chen,[bc] Jong Seung Kim*[a] and Juyoung Yoon*[b]

Received 25th January 2013

DOI: 10.1039/c3cs60024f

www.rsc.org/csr

In the past few decades, the development of optical probes for thiols has attracted great attention because of the biological importance of the thiol-containing molecules such as cysteine (Cys), homocysteine (Hcy), and glutathione (GSH). This tutorial review focuses on various thiol detection methods based on luminescent or colorimetric spectrophotometry published during the period 2010–2012. The discussion covers a diversity of sensing mechanisms such as Michael addition, cyclization with aldehydes, conjugate addition–cyclization, cleavage of sulfonamide and sulfonate esters, thiol–halogen nucleophilic substitution, disulfide exchange, native chemical ligation (NCL), metal complex-displace coordination, and nanomaterial-related and DNA-based chemosensors.

Key learning points

(1) What are the important biological roles of cysteine (Cys), homocysteine (Hcy), and glutathione (GSH)?
(2) What are the design strategies for fluorescent probes which are selective for bio-thiols?
(3) Diversity of sensing mechanisms such as Michael addition, cyclization with aldehydes, conjugate addition–cyclization, cleavage of sulfonamide and sulfonate esters, thiol–halogen nucleophilic substitution, disulfide exchange, native chemical ligation (NCL), metal complex-displace coordination, and nanomaterial-related and DNA-based chemosensors.
(4) Diversity of sensing systems such as small organic molecule based probes, nanomaterial based probes and DNA-based probes, etc.
(5) Diversity of bio-imaging results for these probes and their biological significances.

Introduction

Biological thiols such as those found in cysteine (Cys), homocysteine (Hcy), and glutathione (GSH) play essential roles in human physiology.[1] Cys is a precursor of GSH, acetyl Co-A and taurine, as well as a source of sulfide in iron–sulfur clusters. Abnormal levels of Cys are associated with many human diseases such as slow growth, hair depigmentation, edema, lethargy, liver damage, loss of muscle and fat, skin lesions, and weakness.[2] Hcy is a risk factor for disorders including cardiovascular and Alzheimer's diseases, whereas plasma total Hcy (tHcy) concentration is related to birth defects and cognitive impairment in the elderly.[3] GSH, the most abundant intracellular nonprotein thiol, serves many cellular functions, including maintenance of intracellular redox activities, xenobiotic metabolism, intracellular signal transduction, and gene regulation.[4] More specifically, GSH is the most abundant among the small intracellular molecular thiols (1–10 mM), and a redox homeostasis exists between sulfhydryl (reduced form, GSH) and disulfide (oxidized form, GSSG). It has been revealed that GSH plays a critical role in controlling oxidative stress in order to maintain the redox homeostasis for cell growth and function.[4] Moreover, its level is known to be directly linked to many diseases, including cancer, Alzheimer's, and cardiovascular disease.[5] Therefore, the detection of biomolecular thiols in biological and environmental samples consistently attracts a great deal of attention.

Currently, the most sophisticated analytical techniques for use with thiols include electrochemical detection and high performance liquid chromatography methods (HPLC). However, these instrumentally intensive methods measure only total thiol content, and often require extensive sample preparation for experimental accuracy. Thus, a simple and inexpensive method for not only detecting but also quantifying thiols is essential for real-time monitoring of biological samples.

Among the various methods for detecting thiols, optical techniques, including fluorescence or colorimetric approaches,

[a] *Department of Chemistry, Korea University, Seoul 130-701, Korea. E-mail: jongskim@korea.ac.kr; Fax: +82-2-3290-3121; Tel: +82-2-3290-3143*
[b] *Department of Chemistry and Nano Science and Department of Bioinspired Science (WCU), Ewha Womans University, Seoul 120-750, Korea. E-mail: jyoon@ewha.ac.kr; Fax: +82-2-3277-2384; Tel: +82-2-3277-2400*
[c] *State Key Laboratory of Materials-Oriented Chemical Engineering, College of Chemistry and Chemical Engineering, Nanjing University of Technology, Nanjing 210009, China*

have proven to be some of the most convenient. In particular, fluorescence techniques have a number of advantages, including simplicity, low detection limits, and ease of handling. The most significant benefit to the use of fluorescent probes is the ability to monitor intracellular analytes. With this purpose in mind, during the last couple of decades, great effort has been devoted to the development of fluorescent and colorimetric sensors that are able to selectively sense biological thiols.

Most of the optical probes that recognize thiols utilize two of their characteristic properties: their strong nucleophilicity and their high binding affinity for metal ions. In recent years, the highly selective reactions of thiols in appropriately designed molecular systems have enabled their quantification in both abiotic and natural environments. Since Sippel reported *N*-(4-(7-diethylamino-4-methylcoumarin-3-yl)phenyl)maleimide as one of the first examples of a thiol probe that utilizes the addition reaction of thiols to the maleimide moiety, there have been considerable further achievements.[6] In 2010, we published a thorough review discussing the developments in fluorescent thiol probes up to 2009.[7] Since then, the number of publications regarding this area of research has markedly increased.

In this review, fluorescent and colorimetric sensors are classified according to their mechanism of reaction with thiols. These categories include Michael addition, cyclization with aldehydes, conjugate addition–cyclization reactions, cleavage of sulfonamide and sulfonate esters, thiol–halogen nucleophilic substitution, disulfide exchange, native chemical ligation (NCL), metal complex-displace coordination, and nanomaterial-related and DNA-based chemosensors. Therefore, in this tutorial review we provide a general overview of the selected recent research involving the design and application of biological thiol-selective chemosensors.

Colorimetric and fluorescent methods to detect thiols

Based on Michael addition of thiols

Derivatives of α,β-unsaturated carbonyl moieties are widely used in nucleophilic addition of sulfhydryl groups. In 1970, Kanaoka reported some pioneering work regarding fluorescent thiol chemodosimeters that utilized the addition of a thiol to a maleimide moiety, which is one of the most well known electrophiles.[8]

Recently, Kand *et al.* reported chromenoquinoline-based fluorescent probe **1** for the detection of biological thiols (Fig. 1).[9] In DMSO–HEPES buffer (10 mM, pH 7.4, 1 : 99, v/v), **1** exhibited a 223-fold enhancement in fluorescence intensity on Michael addition of Cys to a maleimide appended to the chromenoquinoline. Probe **1** displayed a linear fluorescence off–on response to biological thiols, and GSH concentration in particular, could be monitored up to 1.46×10^{-8} M. Probe **1** was further investigated for its ability to detect cellular expression of thiols using MDA-MB 231 cells.

Jung *et al.* synthesized coumarin-based chemodosimeter **2** that, based on a Michael-type reaction, could effectively and selectively recognize thiols, showing a preference for Cys over other biologically relevant analytes including Hcy and GSH (Fig. 1).[10] It is known that it is relatively difficult to design a probe *via* a Michael reaction that is selective for Cys over Hcy and GSH. The fluorescence intensity of compound **2** was found to be proportional to the amount of Cys added at the submicromolar level and a detection limit of 30 nM. The pK_a of Cys (8.30) is lower than that of Hcy (8.87) or GSH (9.20). The Cys preference of **2** over Hcy and GSH was also demonstrated by the testing of a metabolite from the HepG2 cell line using LC–MS.

A similar approach was reported by Sun and coworkers. They investigated turn-on fluorescent chemodosimeter **3** for Cys and Hcy that contained a nitroolefin moiety as an electron acceptor (Fig. 2).[11] In CH_3CN–HEPES (0.1 M, pH = 7.4, 1 : 1, v/v), probe **3** exhibited higher selectivity toward biothiols (Cys, Hcy, and GSH) than other amino acids. The reactivity in the order Cys > Hcy > GSH can be rationalized on the basis of steric-hindrance effects on the thiol 1,4-addition reaction. Furthermore, **3** was applied for intracellular thiol imaging in tetrahymena thermophila cells using confocal microscopy analysis.

The fluorescein-based sensor **4**, bearing a nitroolefin moiety, was prepared for the detection of thiols by Wang *et al.* (Fig. 3).[12] Upon addition of a thiol, **4** showed an increase in absorption intensity at 497 nm, with a slight blue-shift as well as an increase in fluorescence intensity at 520 nm. The fluorescence enhancement and absorption changes were attributed to the Michael addition of a thiol to the nitroolefin moiety of the probe. The probe exhibited a fast response to Cys with a rate constant (k_{obs}) of 2.3 min^{-1} and the detection limit was evaluated to be 0.2 μM.

Probe **5** showed selective fluorescence turn-on for biothiols (Cys, Hcy, GSH) (Fig. 4).[13] It exhibited a sensitive and selective

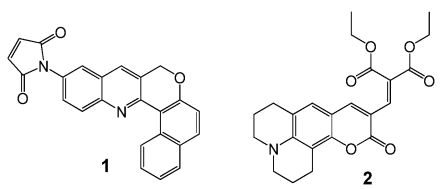

Fig. 1 Structures of probes **1** and **2**.

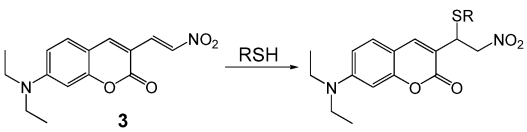

Fig. 2 Michael-type reaction sensing using probe **3**.

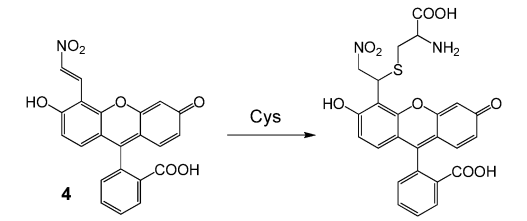

Fig. 3 Schematic illustration of reaction of **4** with thiols.

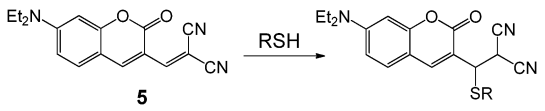

Fig. 4 Proposed reaction mechanism of **5** with thiols.

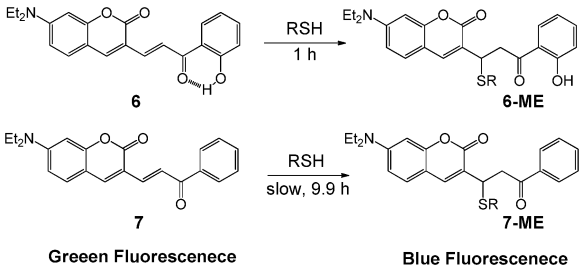

Fig. 5 Reaction mechanism of **6** and **7** for thiol detection.

fluorescence enhancement in the presence of biothiols, which was not observed for other natural amino acids, through the Michael addition of a thiol group to the α,β-unsaturated malonitrile unit of **5**. In DMSO–HEPES buffer (0.1 M, pH 7.4, 1 : 2, v/v), Cys demonstrated a dramatic increase in the fluorescence intensity (F/F_o = 19) compared to other natural amino acids. Hcy and GSH enhanced the fluorescence intensity of **5** by 12- and 5.6-fold, respectively. The probe was then applied for detecting cellular expression and detection of biothiols in HeLa cells.

Kim *et al.* reported on ratiometric fluorescent biothiol probe **6** that was activated by an intramolecular H-bond (Fig. 5).[14] This compound also exhibited sensitive and selective fluorescence enhancement due to biothiols, which was not the case for other natural amino acids. The mechanism of this increase in fluorescence was Michael addition of a thiol group to the α,β-unsaturated unit of **6**. In DMSO–HEPES buffer (0.1 M, pH 7.4, 4 : 1, v/v), the formation of **6**-ME was almost complete within 1 h (half-life τ = 16.5 min) with the second-order rate constant of $k = 6.98 \times 10^{-2}$ M^{-1} s^{-1} at 25 °C, whereas the formation of **7**-ME was very slow (τ = 9.9 h). Probe **6** was also successfully applied to intracellular imaging.

Chemodosimeter **8** was developed by Jung *et al.*, and showed selectivity for Cys over other structurally and functionally similar amino acids, Hcy and GSH. The fluorescence turn-on in the presence of Cys was due to a Michael-type reaction (Fig. 6).[15] The detection process could be carried out under physiological conditions by utilizing the low pK_a of Cys to

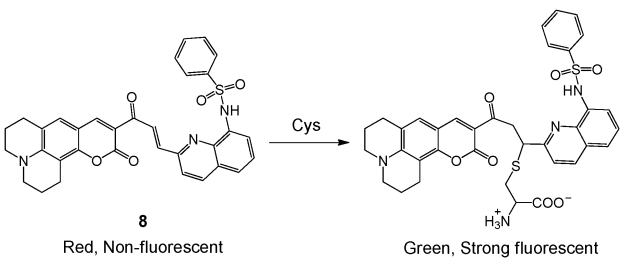

Fig. 6 Chemodosimetric reaction of **8** with Cys.

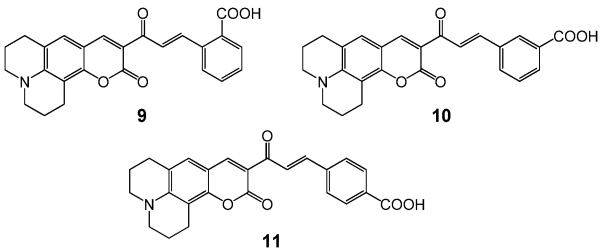

Fig. 7 Structures of Cys probes **9–11**.

generate a stronger nucleophile, and by modifying the hosts in such a way that a larger nucleophile experiences more steric hindrance in reaching the electrophilic center. These points were demonstrated by the fact that the lowest reaction rate constant (highest energy barrier) was for GSH in the second-order reaction and also that the highest interaction energy (calc.) was for GSH. The detection limit for GSH was determined to be 10^{-7} M in aqueous solution. Confocal microscopy experiments demonstrated that **8** could be used in fluorescence imaging of Cys in HepG2 cells.

The same group employed the Michael-type thiol reaction for a series of coumarins (**9–11**), which were able to emit fluorescence in a turn-on manner (Fig. 7).[16] Using fluorescence spectroscopy and DFT calculations, along with kinetic studies, probe **9** was reported to be the most selective for Cys, with a detection limit of 10^{-8} M in phosphate buffered saline (PBS, 10 mM, pH 7.4). This was attributed to the carboxyl group at the *ortho* position on **9** preferring a less negatively charged nucleophile. Probe **9** was also used to assess intracellular Cys in living HepG2 cells.

Chen *et al.* reported the fluorescein-based fluorescent probe **12** for use in the detection of thiol-containing molecules (Fig. 8).[17] Compound **12** gave fluorescence enhancements (λ_{max} = 520 nm) and UV-Vis spectral changes, which were attributed to 1,4-addition of a thiol to the α,β-unsaturated ketone in the molecule, forming a thioether in the presence of thiol-containing analytes (Cys, Hcy, and GSH) in CH_3CN–HEPES buffer (20 mM, pH 7.4, 1 : 99, v/v). **12** showed high sensitivity towards thiols, with a detection limit of 10^{-7}–10^{-8} M, and the observed rate constants (k_{obs}) at pH 7.4 were found to be 36.5, 8.0 and 11.5 min^{-1} for Cys, Hcy, and GSH, respectively.

It was reported by Shiu *et al.* that a Förster resonance energy transfer (FRET)-based iridium(III) complex could be formed with Hcy or Cys on conjugate addition of the thiols to the vinyl sulfide linkage, followed by elimination (Fig. 9).[18] In CH_3CN–PBS (pH = 8.1, 3 : 1, v/v), probe **13** showed high selectivity for Hcy and Cys over other amino acids and GSH. The ratio of

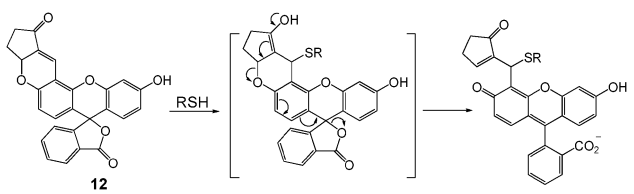

Fig. 8 Schematic illustration of the reaction mechanism of **12** for thiols.

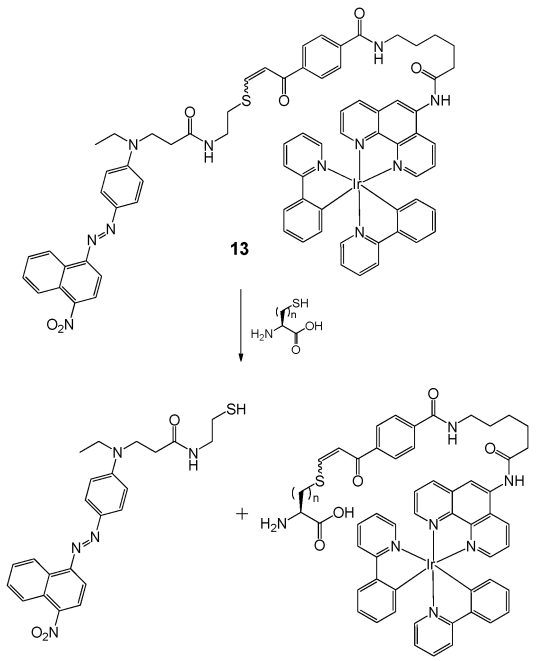

Fig. 9 Proposed reaction mechanism of **13** with thiols.

emission intensity enhancements on the addition of Hcy and Cys was 1.4 : 1. The Ir(III) complex was able to differentiate Hcy from Cys in a ratio of 5 : 1. In addition, **13** could be used for the detection of Hcy and Cys in human blood plasma. The total concentration of Hcy and Cys in the plasma was found to be 0.31 mM; this value is well above the detection limit of probe **13**, *i.e.* 0.12 mM and is within the range of reported concentrations of Hcy and Cys found in normal human blood plasma, *i.e.* 0.25–0.38 mM.

McMahon *et al.* developed a lanthanide based luminescent GSH sensor (Fig 10).[19] Recently, there has been an increased interest in understanding the interactions of iridium(III) complexes with biomolecules as well as the development of these complexes as reagents for biological applications. Lanthanides possess many desirable photophysical properties, such as long wavelength emissions and long-lived excited states, allowing them to be easily distinguished from shorter-lived autofluorescence from biological material. Upon excitation of **14**-Tb at 256 nm (λ_{max} of phenyl antenna) in 20 mM HEPES buffer (pH 7.4), Tb(III) centered emission was observed with bands appearing at 490, 545, 586, and 622 nm. **14**-Tb exhibited a *ca.* 500% enhancement in fluorescence intensity on Michael addition of GSH to a maleimide appended to the Tb(III)–Cyclen. Probe **14**-Tb displayed a linear fluorescence on response to biothiols, and GSH equivalents in particular could be monitored up to 1 equiv. Probe **14**-Tb could also be used for the bio-detection of the GSSG to GSH redox process using glutathione reductase and the reducing agent NADPH in real time by the occurrence of a fluorescence change.

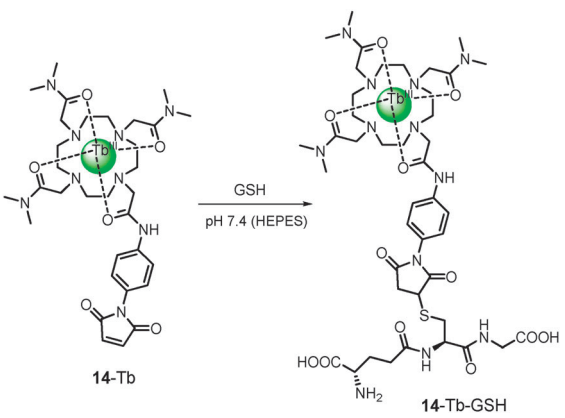

Fig. 10 Reaction of **14**-Tb^{III} with GSH yielding the adduct **14**-Tb^{III}-GSH.

Based on cyclization with aldehydes

The selective reaction of aldehydes with GSH to form thiazolidines has been used in food quality control, environmental science, medicine, and public health analyses. Recently, this chemistry was applied to the detection of Cys and Hcy, as sensors with an aldehyde functionality can form a rapid 6- or 5-membered ring with 1,3- or 1,2-aminothiols, while other biothiols, like GSH, cannot.

Recent work involving this approach was reported by Hu *et al.* (Fig. 11).[20] Probe **15** is weakly fluorescent in the wide physiological pH range of 3–8. Among the various amino acids, only Cys/Hcy induced a fluorescence enhancement at 560 nm with a large absorption peak shift (70 nm) from orange to yellow in CH_3CN–HEPES buffer (20 mM, pH 7.4, 3 : 7, v/v). The fluorescence intensities of **15** showed a good linear relationship with the concentration of Cys, using physiological levels ranging from 0 to 500 μM. Its detection limit for Cys was 6.8×10^{-7} M. Compound **15** could also be used for the bioimaging of Cys/Hcy in living cells, and for detection in human plasma by the occurrence of a visible color change.

Liu *et al.* reported the biocompatible phosphorescent nanoprobe **16** for Cys and Hcy detection, which used mesoporous silica nanoparticles as carriers and an Ir(III) complex as a signaling unit (Fig. 12).[21] In PBS solution (pH 7.4), only Cys and Hcy induced a double-signal response of turn-on phosphorescence at 531 nm,

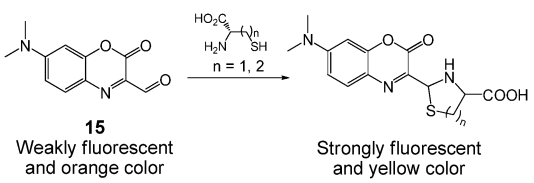

Fig. 11 Proposed reaction mechanism of **15** with Cys and Hcy.

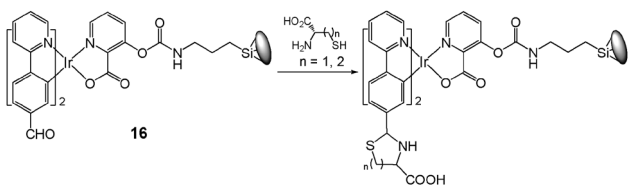

Fig. 12 Reaction mechanism of **16** towards Cys and Hcy.

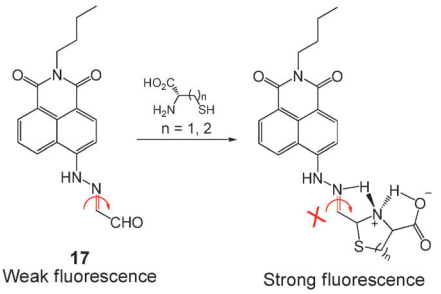

Fig. 13 Schematic illustration of reaction of **17** with Cys and Hcy.

and emission color changes from orange to bright green, which could be observed by the naked eye. Moreover, cytotoxicity and confocal scanning microscopy experiments indicated that nanoprobe **16** had good biocompatibility and was able to penetrate cell membranes, facilitating fast phosphorescence bioimaging of Cys and Hcy in live cells.

Wang *et al.* reported the naphthalimide-based glyoxal hydrazone **17** for the fluorescence turn-on detection of Cys and Hcy, based on inhibition of C=N isomerization-induced quenching by an intramolecular hydrogen bond (Fig. 13).[22] The cyclization reaction with Cys and Hcy was assumed to block the isomerization quenching by forming an intramolecular hydrogen bond with the lone pair of electrons on the nitrogen of the ring thiazolidine, increasing the fluorescence intensity of **17** in DMSO at 524 nm. Moreover, in DMSO–HEPES buffer (100 mM, pH 7.4, 1 : 1, v/v), dose-dependent fluorescence enhancement of probe **17** showed good linearity in the Cys and Hcy concentration range of 0–500 μM. This compound was successfully applied to the biological imaging of Cys or Hcy inside living cells.

Based on conjugate addition–cyclization reaction with Cys/Hcy

Research in this area has provided some promising probes that are selective for Cys and Hcy. However, the ability to distinguish between the two using a single probe remains a significant challenge. This is because of the structural similarity of Cys and Hcy, which only differ by a single methylene unit in their side chains.

In 2011, Yang *et al.* reported benzothiazole derivative **18** for the detection of Cys and Hcy in neutral media (Fig. 14).[23] The method involved thioether formation followed by cyclization to

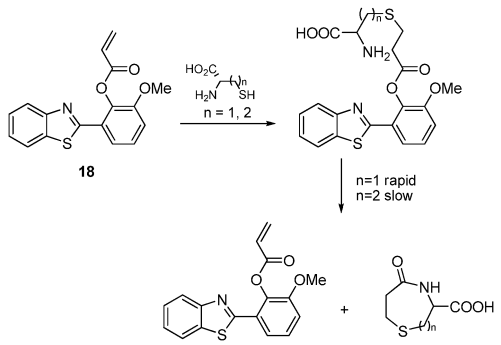

Fig. 14 Thiol sensing profile of **18** towards Cys/Hcy.

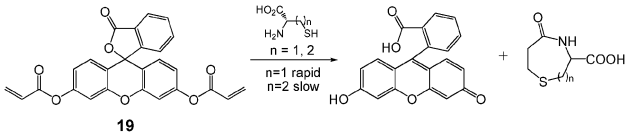

Fig. 15 Schematic illustration of reaction of **19** with Cys/Hcy.

produce 2-(2′-hydroxy-3′-methoxyphenyl)benzothiazole (HMBT) and a lactam. The differences in ring-formation kinetics allowed spectral or kinetic modes to be used to separately identify Cys and Hcy. In addition, the simultaneous detection of Cys and Hcy in diluted deproteinized human plasma was carried out successfully.

Wang *et al.* reported the off–on fluorescent chemodosimeter **19** for discriminative detection of Cys (Fig. 15).[24] Incubation with 50 μM Cys in an EtOH–phosphate buffer (20 mM, pH 7.4, 2 : 8, v/v) for 10 min, resulted in the appearance of a new absorption band centered at 490 nm, accompanied by a remarkable fluorescence enhancement at 515 nm. If the incubation time was kept to 10 min, **19** exhibited high selectivity for Cys over Hcy. The fluorescence enhancement and UV-vis spectral changes induced by Cys were attributed to the adduct–addition reaction between Cys and the acryloyl group in the probe, followed by the cleavage of the ester bond to form the fluorescein. Interestingly, double acrylate-containing sensor **19** indicated a remarkable enhancement in selectivity for Cys over Hcy, compared with the single acrylate-containing fluorescein derivate **19**. It was reasoned that the dual addition–cleavage processes in the reaction between **19** and Cys led to the enhancement in selectivity.[24]

Guo *et al.* designed ratiometric near-infrared (NIR) cyanine-based probe **20** for detection of Cys with high selectivity over Hcy and GSH (Fig. 16).[25] The probe possessed an acrylate group as a functional trigger moiety for the thiol. Upon addition of Cys, an adduct–cyclization reaction induced the formation of hydroxyl cyanine, followed by tautomerization to produce **20′**. Accordingly, the solution containing **20** showed remarkable shifts in the absorption and emission spectra (from 770 to 515 nm for absorption and from 780 to 570 nm for emission). The selective response for Cys was attributed to the differences in the rate of the adduct–cyclization reaction between **20** and the different thiols. Probe **20** was further applied to biological imaging of Cys inside living cells. **20** showed a strong fluorescence at 590 nm and a sharp fluorescence decrease in the NIR region (760–855 nm) for MCF-7 cells grown in glucose-free Dulbecco's modified Eagle medium. It is known that the intracellular Cys level is significantly increased during glucose deprivation in parental MCF-7 cells. Probe **20** successfully

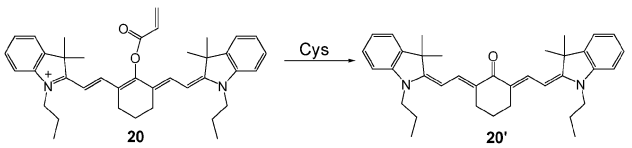

Fig. 16 Reaction mechanism of **20** with Cys/Hcy.

displayed nice ratiometric imaging of *in vivo* Cys using two different imaging signal channels.

Based on cleavage of sulfonamide and sulfonate esters by thiols

Nucleophilic substitution of sulfonate esters and amides of fluorescent phenols or amines has been used for the development of chemodosimeters for the detection of thiols. Ji *et al.* reported the off–on red-emitting phosphorescent thiol probe **21** (Fig. 17).[26] In CH_3CN–water (4 : 1, v/v) solution, **21** was non-luminescent because the metal to ligand charge transfer (MLCT) was corrupted by electron transfer from Ru(II) to an intramolecular electron sink (2,4-dinitrobenzenesulfonyl). Thiols were able to cleave the electron sink, and the MLCT was re-established. Phosphorescence at 598 nm was enhanced by 90-fold, with a 143 nm (5256 cm^{-1}) Stokes shift and a 1.1 μs luminescence lifetime.

Yuan *et al.* reported a new class of NIR fluorescent dyes that are superior to traditional 7-hydroxycoumarin and fluorescein, with both absorption and emission in the NIR region while retaining an optically tunable hydroxyl group (Fig. 18).[27] In addition, they performed quantum chemical calculations with the B3LYP exchange function, employing 6-31G(d) basis sets in order to elucidate the structure–optical properties of this new class of NIR dyes. Compound **22**, upon addition of Cys at pH 7.4 (PBS–CH_3CN (7 : 3)), showed a dramatic change in the fluorescence spectra. A strong new emission peak appeared at 716 nm, with a 50-fold enhancement. Furthermore, the authors demonstrated that **22** was suitable for NIR fluorescence imaging of thiols in RAW 264.7 macrophage cells, as well as *in vivo*.

Jiang *et al.* reported the turn-on fluorescent NIR probe **23** for Cys detection (Fig. 19).[28] Cleavage of 2,4-dinitrobenzenesulfonyl (DNBS) with thiols switched the weakly fluorescent aza-BODIPY dye (λ_{em}=734 nm, Φ_f = 0.03) to a strongly fluorescent species in the NIR region (λ_{em} = 755 nm, Φ_f = 0.14) in CH_3CN–H_2O–DMSO (pH 7.5, 79 : 20 : 1, v/v/v). Probe **23** showed good specificity toward Cys over other biological molecules, and the detection limit was determined to be 5×10^{-7} M.

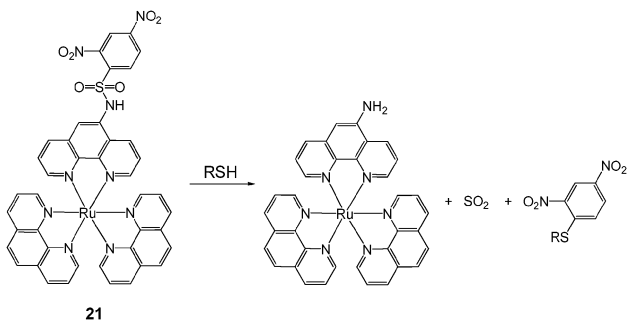

21

Fig. 17 Thiol sensing mechanism of **21**.

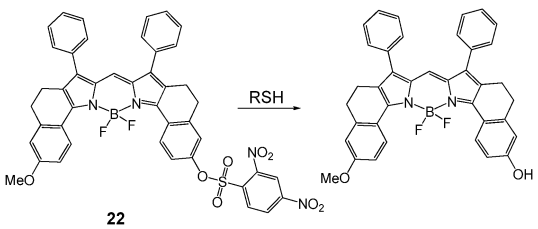

22

Fig. 18 Schematic illustration of the reaction of **22** with thiols.

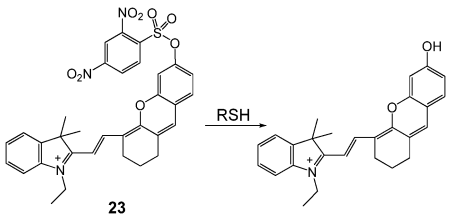

23

Fig. 19 Schematic illustration of the reaction of **23** with thiols.

Based on thiol–halogen nucleophilic substitution by thiols

A great deal of research involving the sensing of biologically active thiols has been published. However, the discrimination between GSH and the two amino acids, Cys and Hcy, using a single probe has remained a significant challenge to chemists because of their structural similarity and the reactivity of the thiols.

In this regard, Niu *et al.* recently developed the BODIPY-based ratiometric fluorescence sensor **24**, which could effectively and selectively recognize thiols based on a rapid displacement of chloride with thiolate, showing a discrimination between GSH and Cys/Hcy (Fig. 20).[29] The chlorine of the monochlorinated **24** could be rapidly displaced by the thiolate of biothiols through thiol–halogen nucleophilic substitution. The amino groups of Cys/Hcy, but not GSH, could further replace the thiolate to form an amino-substituted probe. In aqueous HEPES buffer (20 mM, pH 7.4) containing 5% acetonitrile, the fluorescence intensity of **30** was found to be proportional to the amount of GSH added in the 0–60 μM range, with a coefficient of R = 0.993 and a detection limit of 8.6×10^{-8} M (S/N = 3). Confocal microscopy experiments demonstrated that **24** has potential for the ratiometric imaging of GSH in HepG2 cells.

Based on disulfide exchange reaction by thiols

Lee *et al*. reported the two-photon fluorescent probe **25** towards the detection of thiols deep inside living tissues (Fig. 21).[30]

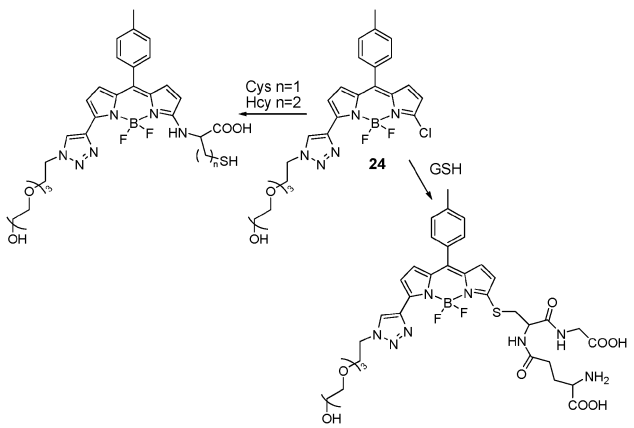

Fig. 20 Reaction mechanism of **24** for thiols.

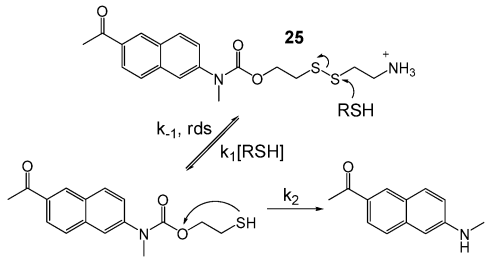

Fig. 21 Reaction mechanism of **25** for thiols.

In MOPS buffer solution (pH 7.2), addition of thiols induced a rate-limiting attack of the thiol at the disulfide bond followed by the cleavage of the C–N bond to afford **25** without any significant interference from other biologically relevant analytes. Probe **25** gave a 10-fold two-photon excited fluorescence (TPEF) intensity enhancement in response to thiols, which was pH-insensitive at biologically relevant pH, and emitted 11-fold stronger TPEF than **25** alone. Disulfide bond cleaved **25** could be observed both in HeLa cells and in rat hippocampal tissues at depths of 90–180 μm.

Lim *et al.* reported the ratiometric two-photon (TP) probe **26** for mitochondrial thiol detection (Fig. 22).[31] Mitochondrial GSH (mGSH) exists predominantly in the reduced form, with a GSH : GSSG ratio of >100 : 1. An increase in the GSSG-to-GSH ratio is considered to be indicative of oxidative stress conditions. To understand the roles of RSH in biology, it is crucial to monitor RSH at the cell, tissue, and organism level. This probe had 6-(benzo[*d*]thiazol-2′-yl)-2-(*N*,*N*-dimethylamino)naphthalene as a TP fluorophore, a disulfide group as a thiol-reactive site, and triphenyl phosphonium salt (TPP) as the mitochondrial targeting group. Probe **26** selectively stained the mitochondria over other organelles of HeLa cells, with ratiometric emissive color changes from blue (F_{blue} 425–475 nm) to yellow (F_{yellow} 525–575 nm) in the presence of cellular thiols. Upon excitation at 740 nm, the image ratio (F_{yellow}/F_{blue}) of HeLa cells with **26** was 1.24. Probe **26** could detect mitochondrial thiols in live cells and living tissues at a depth of 90–190 μm.

Lee *et al.* reported the single galactose-appended naphthalimide **27** as a probe for hepatic thiol imaging in living cells and animals (Fig. 23).[32] The galactose subunit in **27** served to guide the probe to hepatocytes, while the disulfide-linked naphthalimide moiety provided fluorescence emission at 540 nm when exposed to cellular thiols, as a result of disulfide cleavage. The mechanism

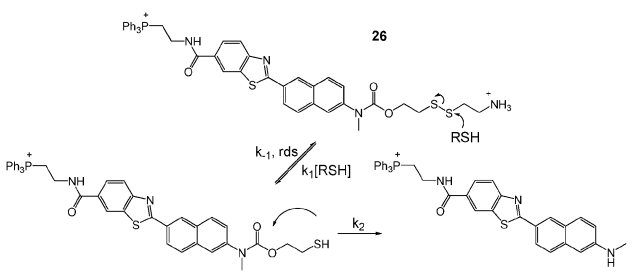

Fig. 22 Schematic illustration of the reaction of **26** towards thiols.

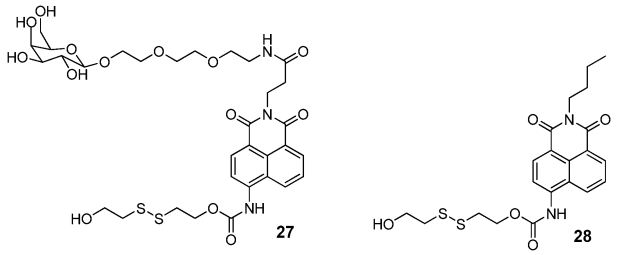

Fig. 23 Structures of probes **27** and **28**.

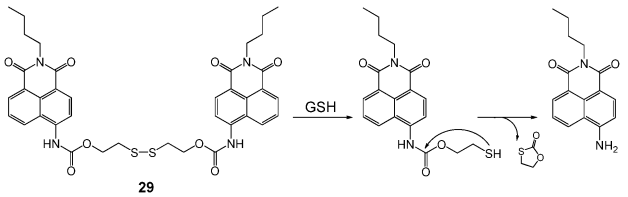

Fig. 24 Disulfide bond cleavage mechanism in **29** towards thiols.

was deduced using experiments with analog **28** without galactose, which showed no selectivity for any particular organs.

Zhu *et al.* reported a naphthalimide-based ratiometric fluorescent probe, containing a disulfide group (Fig. 24).[33] When GSH was added to a solution of **29** in EtOH–PBS (20 mM, pH 7.4, 1 : 9, v/v), the maximum absorption peak showed an 85 nm red-shift and the color of the solution turned from colorless to jade-green. The maximum emission peak underwent a red-shift of 48 nm, and the ratio of fluorescence intensities (F_{533}/F_{485}) changed from 0.5 to 5.7. Furthermore, **29** allowed the determination of GSH using a ratiometric fluorescence method with a detection limit of 28 μM, and more importantly, distinct ratiometrical fluorescence changes of **29** were observed in HeLa cells.

Ding *et al.* reported a strategy of photoelectrochemical (PEC) analysis with chemiluminescence (CL) of the isoluminol–H_2O_2–Co^{2+} system as a light source for the determination of physiological thiols in cancer cells (Fig. 25).[34] Polystyrene microspheres (PSMs) bearing isoluminol and thiolated DNA were attached to the surface of magnetic beads to form **30**. In the presence of thiols, the disulfide bonds in **30** were cleaved. The isoluminol molecules present on the surface of the PSMs were detached by magnetic separation and transferred to a dark cell for PEC detection. The relatively low detection limit of 42 pM and a broad dynamic range of GSH of 1.0×10^{-10} M–1.0×10^{-8} M were achieved.

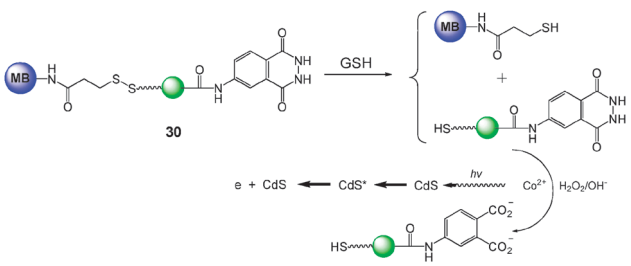

Fig. 25 Proposed reaction mechanism of **30** for thiols.

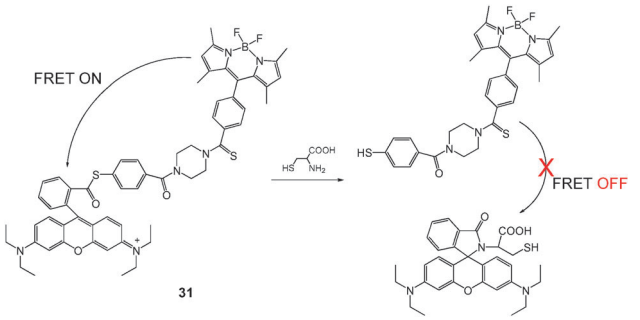

Fig. 26 Structure of ratiometric fluorescent thiol probe **31** based on the NCL reaction.

Based on the native chemical ligation (NCL) mechanism for aminothiols

The native chemical ligation (NCL) reaction has attracted significant attention in the fields of chemistry and biology. Hundreds of proteins have been prepared by total or semi-synthesis using this reaction. NCL of peptide segments involves cascade reactions between a peptide-α-thioester and an N-terminal cysteine peptide.

Prompted by the chemoselective and biocompatible characters of the NCL reaction, Long *et al*. prepared the ratiometric fluorescent probe **31** for thiol detection on the basis of a FRET signaling mechanism (Fig. 26).[35] Owing to the overlap of the emission band of the BODIPY with the absorption band of the rhodamine in probe **31**, excitation at 470 nm displayed remarkable emission of the rhodamine at 590 nm, but the BODIPY emission at 510 nm remained completely quenched in 25 mM CH_3CN–phosphate buffer (pH 7.4, 9 : 11, v/v). Upon addition of Cys to a solution of **31**, the rhodamine emission band at 590 nm was gradually reduced with a concomitant increase in the emission band of the BODIPY at 510 nm. There was a 270-fold enhancement in the emission ratio (I_{510}/I_{590}) with a detection limit of 82 nM towards Cys. Moreover, confocal microscopy experiments demonstrated that **31** has the potential to be used in the ratiometric imaging of Cys in living HeLa cells.

Based on cleavage of Se–N by thiols

Selective cleavage of the Se–N bond by strong nucleophilic thiols was adopted for the design of a thiol probe by Zhu *et al*. (Fig. 27).[36] The pyridylvinylene derivative containing piazselenole **32** displayed a 19 nm red-shift in absorption spectra and a ~3-fold fluorescence intensity enhancement at 440 nm with

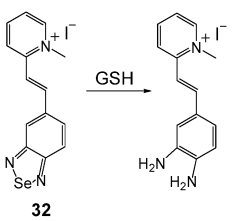

Fig. 27 Reaction of **32** with GSH.

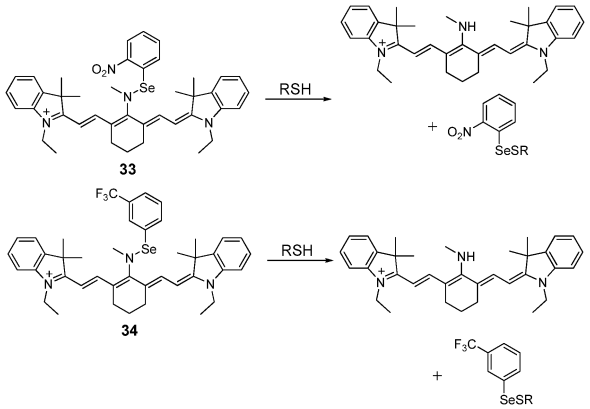

Fig. 28 Reaction mechanisms of probes **33** and **34** with thiols.

GSH in a mixture of DMF–H_2O (8 : 2, v/v) solution. Probe **32** exhibited a linear relationship between absorbance/fluorescence and concentration of GSH in the range of 4–12 μM and 2–12 μM, respectively, and a detection limit of 0.03 μM.

Recently, Wang *et al*. reported the sensitive NIR fluorescent thiol probes **33** and **34** (Fig. 28).[37] Because of a donor-excited photo-induced electron transfer (d-PET) process occurring between the modulator and the fluorophore, upon excitation at 635 nm, probes **33** and **34** displayed weak fluorescence at 750 nm after incubation at 25 °C for 3 min in PBS (15 mM, pH 7.4). Upon addition of GSH to the solutions of **33** and **34**, the emission band of the free dyes at 750 nm exhibited a significant fluorescence enhancement. Moreover, the fluorescence intensities of **33** and **34** were proportional to the amount of Cys added in the 0–5 μM range. Confocal imaging confirmed that the two compounds could be used for detecting thiols in living RAW 264.7 cells and fresh rat liver tissues.

Metal complex related: displacement of coordination by thiols

A nucleophilic displacement approach that utilizes the high affinity of thiols towards metal ions has also been used for developing chemodosimeters for thiols.

Jung *et al.* reported an iminocoumarin–Cu^{2+} ensemble probe for the detection of thiols (Fig. 29).[38] In 10 mM PBS solution (pH 7.4, 1.0% DMSO), only the thiol-containing amino acids induced an enhancement in fluorescence and a red to green color change from among a variety of molecules. The detection limit for GSH was determined to be 10^{-8} M in aqueous solution. Confocal microscopy experiments demonstrated that **35**–Cu^{2+} had potential for use in the imaging of thiols in HepG2 cells.

The iminofluorescein–Cu^{2+} ensemble probe **36** was prepared by Wang *et al.* for the detection of thiols in aqueous solution (Fig. 30).[39] It was proposed that the addition of Cys induced decomplexation of Cu^{2+} from the weakly fluorescent ensemble, which was followed by hydrolytic cleavage of the resulting Schiff base to give a strongly fluorescent fluoresceinaldehyde. Through fluorescence titration, the detection limit of the ensemble probe was evaluated to be 9 μM for Cys.

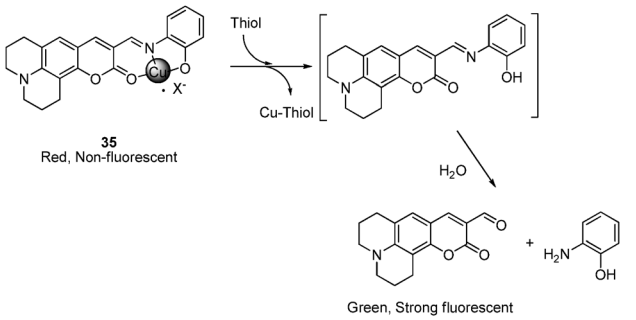

Fig. 29 Schematic illustration of the thiol detecting the chemodosimetric mechanism of **35**–Cu^{2+} in aqueous media.

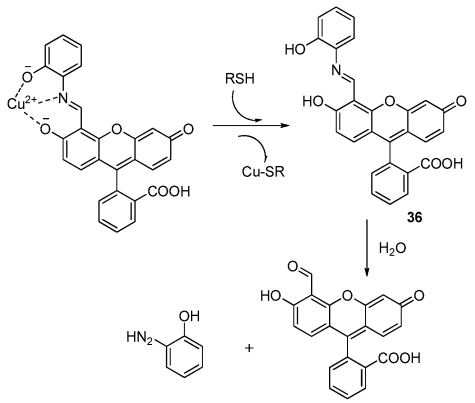

Fig. 30 A plausible mechanism for response of **36**–Cu^{2+} to thiols.

Ruan *et al.* reported a specifically Hg^{2+}-mediated perylene bisimide (PBI) chemosensor for Cys, based on the aggregation of the PBI Cys (Fig. 31).[40] A 0.33 μM concentration of PBI in DMF–H_2O (9 : 1 v/v) showed a fluorescence band at 532 nm, corresponding to the typical monomer emission. Upon the addition of Hg^{2+}, this band decreased because of the aggregation of PBI like "thymine–Hg^{2+}–thymine" (T–Hg^{2+}–T) structure. When Cys was added, the Hg–S bond was able to form instead

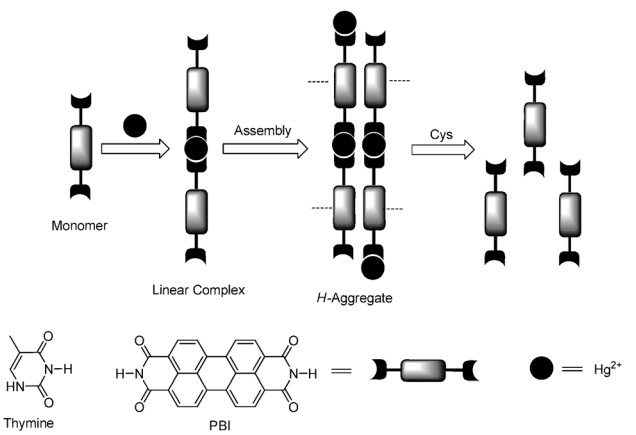

Fig. 31 Scheme of Hg^{2+} induced aggregation of PBI and aggregate dissociation in the presence of Cys.

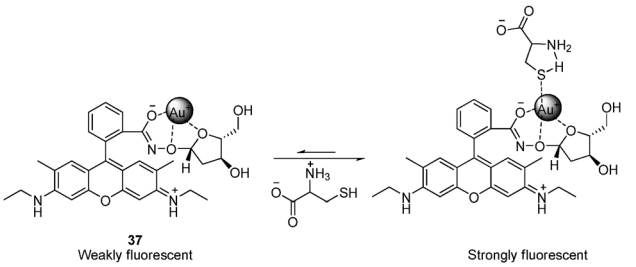

Fig. 32 A proposed structure of the ternary complex of **37**–Au^{+} with Cys.

of T–Hg^{2+}–T, inducing the formation of PBI monomers, which led to the fluorescence enhancement. On increasing the concentration of Cys, there was a linear relationship between fluorescence intensity and concentration in the range 0.05–0.3 μM, with a detection limit of as low as 9.6 nM. This sensor had high selectivity for thiol-containing amino acids over others.

Yang *et al.* reported the turn-on fluorescence probe **37**, based on a rhodamine–Au–sugar complex, for detecting Cys and Hcy (Fig. 32).[41] When various amino acids were added to the **37**–Au^{+} complex in H_2O (1% MeOH), only Hcy and Cys led to a fluorescence increase and a color change from colorless to red. The binding stoichiometry between **37**–Au^{+} and Cys was found to be 1 : 1, and the binding constant in H_2O (1% MeOH) was calculated to be 6.65×10^3 M^{-1}. Fluorescence titration experiments showed that the detection limit for Cys was at the 100 nM level.

Based on a water-soluble conjugated polymer **38**, Kwon *et al.* reported a highly selective probe for detecting Cys in aqueous solution (Fig. 33).[42] Initially, the sensor was assembled as a polymer–Hg^{2+}–thymine complex *via* specific binding of Hg^{2+}–thymine and Hg^{2+}–S in the polymer. Accordingly, the emission moved from 420 nm to 653 nm because of the formation of solid aggregates. Upon the addition of Cys, the stronger binding of Hg^{2+} towards Cys induced the dissociation of the ensemble, which produced a water-soluble polymer, leading to the recovery of blue emission. The limit of detection was estimated to be 6.0×10^{-5} M. Furthermore, this system was used for the imaging of Cys in Zebrafish.

Through Suzuki condensation, Bao *et al.* synthesized two conjugated polymers (**39** and **40**) containing 2,2-biimidazole moieties (Fig. 34).[43] After binding with Ag^{+}, both polymers exhibited a red-shift of 40 nm with a reduced intensity at 416 nm. Upon addition of Cys, the polymer–Ag^{+} was dissociated, releasing free polymers owing to the stronger binding between Cys and Ag^{+}. Correspondingly, **39**–Ag^{+} exhibited emission enhancement with a blue-shift from 456 nm to 416 nm.

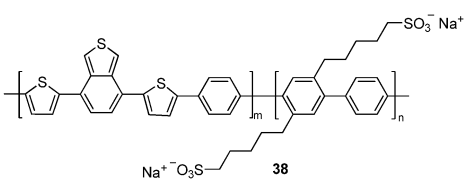

Fig. 33 Structure of polymer **38**.

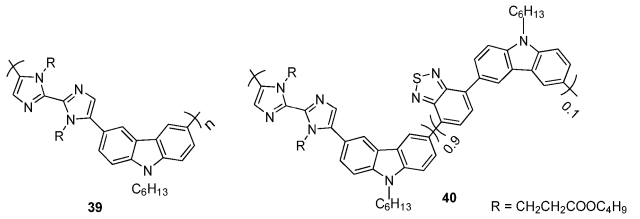

Fig. 34 Structures of **39** and **40**.

By correlating the ratio of emission intensities (F_{416}/F_{456}) with the concentration of Cys, the limit of detection of **39**–Ag^{+} for Cys was as low as 90 nM. Similarly, the limit of detection of **40**–Ag^{+} for Cys was evaluated to be 150 nM.

Nano-material related

Recently, gold nanoparticles (AuNPs) have received a great deal of attention in analytical chemistry fields.

Xu *et al.* reported a colorimetric assay for detecting biothiols based on Hg^{2+}-mediated aggregation of AuNPs (Fig. 35).[44] Hg^{2+} can induce aggregation of thiol-containing naphthalimide-capped AuNPs, accompanied by a color change from red to blue, because of the formation of a structure analogous to the T–Hg^{2+}–T, mentioned earlier. An absorption band at 600 nm emerged, with a blue color corresponding to the aggregated AuNPs. Because of the higher affinity of Hg^{2+} for biothiols, AuNPs were dispersed by their addition, leading to a color change from blue to red, a decrease in the absorption band at 610 nm, and an increase in that at 528 nm. A good linear relationship was observed between the absorbance ratios of A_{528}/A_{615} and the concentration of thiols in the range of 0.025–2.28 μM for GSH, 0.035–1.53 μM for Cys, and 0.04–2.20 μM for Hcy. The detection limits of this assay for GSH, Cys, and Hcy were 17 nM, 9 nM, and 18 nM, respectively. Using Cys as the standard, the total biothiol content in human urine was

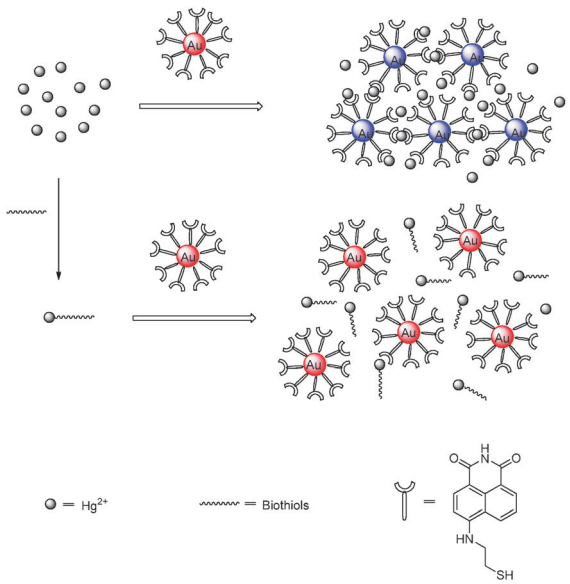

Fig. 35 Schematic illustration of Hg^{2+}-mediated aggregation of AuNPs for colorimetric sensing of biothiols.

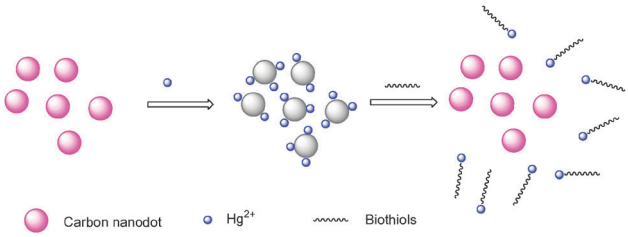

Fig. 36 Schematic illustration of the detection mechanism of Hg^{2+} and biothiols using the carbon nanodots.

determined successfully by the Hg^{2+}-mediated aggregation of AuNPs. No significant interference for the thiol determination was observed in urine samples in that the recoveries ranged from 93.4% to 105.8%.

Zhou *et al.* reported a novel unmodified carbon nanodot (C-Dot) fluorescence probe for detecting Hg^{2+} and biothiols (Fig. 36).[45] Hg^{2+} can induce the fluorescence quenching of the C-Dots owing to a charge transfer process. The emission peak of C-Dots appeared at 410 nm and the quantum yield decreased from 11% to 8.9%. After the addition of thiols, Hg^{2+} was displaced from the surface of the C-Dots because of the formation of Hg^{2+}–S bonds. A good linear relationship between the enhancement of fluorescence and the concentration of Cys in the range of 0.01–5 μM was observed, and the detection limit was calculated to be 4.9 nM. Only biothiols were able to induce the increase in fluorescence, compared to other amino acids, at a concentration of 5 μM, demonstrating the good selectivity of the system for thiols. The determination of biothiols was also carried out in fetal bovine serum (FBS) for evaluating the applicability of the present sensing assay in biological samples. The total biothiol content was determined by the standard addition method using Cys as the standard. The method provided good recoveries ranging from 96.1% to 104.9%, indicating great potential for detecting thiols in practical sample analysis.

Recently, a new spectral technique, resonance light scattering (RLS),[46] has been used for the determination of aminothiols or thiol-containing pharmaceutical compounds. The light scattering signal is relative to the aggregation or assembly of samples, and can be easily detected using a conventional spectrofluorometer by simultaneously scanning both the excitation and emission monochromators.

Using polyethyleneimine-capped Ag-nanoclusters as the probe, Sun *et al.* reported an RLS method for discriminating between Hcy and other biothiols (Fig. 37).[46] Compared with Cys, GSH, and other amino acids, the stronger reducing ability of Hcy favors the reaction with Ag-nanoclusters. In addition, the carboxyl groups of Hcy can electrostatically bind to the amino groups of polyethyleneimine. Thus, Hcy serves as a linker between the Ag cores and hyperbranched polyethyleneimine, inducing the assembly of Ag-nanoclusters and producing the RLS signal. Through monitoring the RLS intensity at 630 nm with increasing concentrations of Hcy, the detection limit was evaluated to be 42 nM. The Hcy determination assay was carried out in human serum samples for demonstrating the applicability

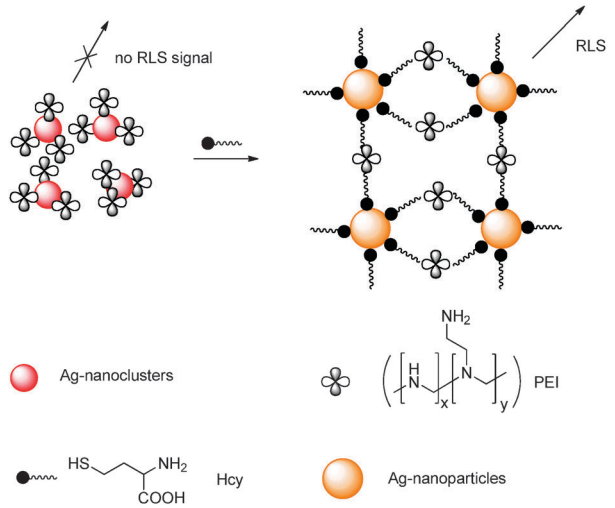

Fig. 37 Schematic illustration of Hcy-involved assembly of PEI-capped Ag-nanoclusters.

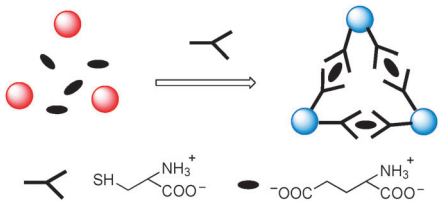

Fig. 38 Aspartic acid-promoted colorimetric sensing of Cys using Au-NPs.

of the present sensing system. In the ultrafiltrated serum samples, the spiked Hcy was quantified with the recoveries ranging from 96% to 112%, indicating great potential for detecting Hcy in biological fluids.

Qian *et al.* reported a AuNP probe for selective detection of Cys (Fig. 38).[47] The AuNP dispersion in aqueous solution displayed a red color and an absorption peak centered at 520 nm. Interestingly, the addition of Cys or Asp alone did not cause any optical changes; however, upon addition of Cys to a AuNP dispersion containing Asp, the NPs aggregated owing to the ion pair interaction between the two amino acids at the particle–solution interface, affording a color change from red to blue. The detection limit for Cys was calculated to be 100 nM. Most importantly, this sensing system showed a good selectivity for Cys over other amino acids and other thiols, including Hcy and GSH. When the Au-NP dispersion containing aspartic acid was added to the brain microdialysate of adult male rats, the changes in the absorption spectrum were similar to those observed upon the addition of Cys. The level of Cys in rat brain microdialysates was evaluated to be 9.6 ± 2.1 μM according to the calibration curve. The result indicated that the present system is effective to selectively sense Cys in the cerebral system.

Guan *et al.* reported a sensory system for detecting Cys and GSH based on band-selective coupling-induced enhancement of two-photon photoluminescence in gold nanocubes (AuNCs) (Fig. 39).[48] When Cys or GSH was added, the X-band photoluminescence

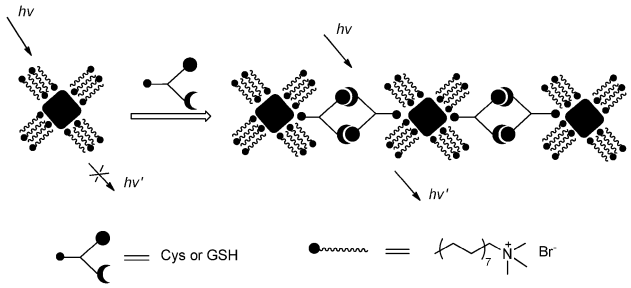

Fig. 39 Assembly mechanism of gold nanocubes induced by Cys/GSH.

intensity of AuNCs under two-photon excitation was increased 60-fold and 46-fold, respectively, owing to the formation of an AuNC assembly. The detection limit was evaluated to be 0.5 μM for Cys and 1.3 μM for GSH. Given the advantages of two-photon near-infrared excitation including high tissue penetration, localized excitation, less tissue autofluorescence and reduced photodamage, the present system possessed potential application in imaging biothiols *in vivo*.

DNA utilized chemosensors

Based on a thiazole orange (TO)/DNA/metal ion ensemble, Pu *et al.* reported a new system for detecting Cys and His with high sensitivity and selectivity, and a rapid fluorescence turn-on response (Fig. 40).[49] Initially, TO/DNA was strongly fluorescent, but the addition of metal ions such as Hg^{2+} or Cu^{2+} resulted in fluorescence quenching. When Hg^{2+} was used as the metal ion, the ensemble exhibited a high selectivity for Cys over other amino acids. However, when the metal ion was Cu^{2+}, both Cys and His induced the fluorescence turn-on response. Most importantly, the detection range of the ensemble could be tuned by adjusting the concentration of metal ions. Through monitoring the fluorescence emission spectra of TO/DNA containing Hg^{2+} ([TO] = 5×10^{-7} M, [DNA] = 5×10^{-8} M, [Hg^{2+}] = 6.25×10^{-7} M), a linear relationship between the enhanced fluorescence intensity and the Cys concentration in the range of 2.5×10^{-9} to 1.1×10^{-7} M was observed, and the detection limit of Cys was evaluated to be 5.1×10^{-9} M.

Xie *et al.* reported a novel fluorescence sensor for Cys detection based on graphene oxide (GO), Ag^{+}, and cytosine (Fig. 41).[50] In the absence of Ag^{+}, the unfolded ssDNA was adsorbed on the surface of GO by stacking interactions between

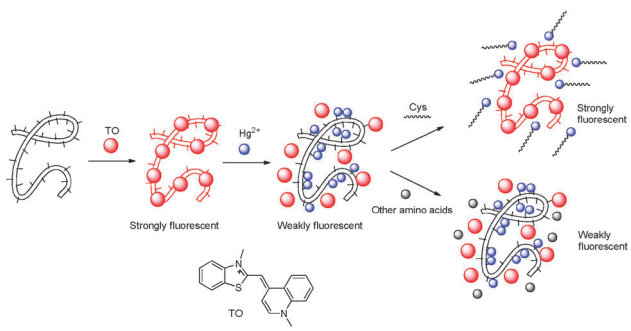

Fig. 40 Schematic illustration of the TO/DNA/metal ion-based amino acid sensor.

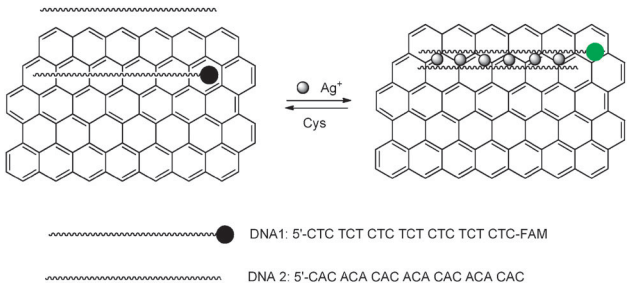

Fig. 41 Schematic representation of Ag^+ and Cys detection based on graphene oxide and silver-specific oligonucleotides.

nucleotide bases and GO, leading to the fluorescence quenching of fluorescein derivative (FAM)-labeled DNA1. Upon the addition of Ag^+, a complex of C–Ag^+–C was formed, inducing an increase in fluorescence as well as a red-shifted emission. When Cys was added, the C–Ag^+–C complex could decompose because of the stronger binding between Cys and Ag^+. Fluorescence quenching was again observed, and the emission returned to the original wavelength. By monitoring the quenching of the fluorescence, the detection limit for Cys was estimated to be 44 nM.

Concluding remarks

In this review, we have discussed a series of luminescent and colorimetric sensors for thiol detection that have been recently reported. Exciting progress has been made during the past few decades in thiol detection and the biological application of the developed methodology. Among the various organic thiols that exist, we mainly focused on the thiol-containing amino acids Cys, Hcy, and GSH, which are similar in their structures and reactivities. A particularly interesting aspect is the ability to distinguish between these three thiols, a challenge that has received a lot of attention for biological applications. We herein classified the developed fluorescent and colorimetric sensors based on the nature of the reaction mechanisms of the probes towards the thiols. For biosensing applications, syntheses of compounds that bear NIR fluorophores, in addition to a unit that can be used to target the probe to a specific organ or cell organelle for drug delivery systems (DDS), are now in progress in many research groups. In most fluorogenic sensor systems, including prodrugs, nanocapsules, hydrogels, and hybrid nanoparticles, it is highly advantageous to have switch-on type or clear-cut ratiometric changeable fluorescence probes to enable clear observation of the change in fluorescence. Many chemists are actively involved in this promising project, and hence, the discovery of a highly efficient and advanced molecular probe for thiol sensing could be very near.

Acknowledgements

J.Y. acknowledges the CRI project (2012R1A3A2048814), J.S.K. acknowledges the CRI project (20120000243), and X.C. acknowledges the NSFY of China (21002049).

Notes and references

1 S. Y. Zhang, C.-N. Ong and H.-M. Shen, *Cancer Lett.*, 2004, **208**, 143–153.
2 S. Shahrokhian, *Anal. Chem.*, 2001, **73**, 5972–5978.
3 S. Seshadri, A. Beiser, J. Selhub, P. F. Jacques, I. H. Rosenberg, R. B. D'Agostino, P. W. F. Wilson and P. A. Wolf, *N. Engl. J. Med.*, 2002, **346**, 476–483.
4 T. P. Dalton, H. G. Shertzer and A. Puga, *Annu. Rev. Pharmacol. Toxicol.*, 1999, **39**, 67–101.
5 W. A. Kleinman and J. P. Richie, *Biochem. Pharmacol.*, 2000, **60**, 19–29.
6 T. O. Sippel, *J. Histochem. Cytochem.*, 1981, **29**, 314–316.
7 X. Chen, Y. Zhou, X. Peng and J. Yoon, *Chem. Soc. Rev.*, 2010, **39**, 2120–2135.
8 Y. Kanaoka, M. Machida, K. Ando and T. Sekine, *Biochim. Biophys. Acta*, 1970, **207**, 269–277.
9 D. Kand, A. M. Kalle, S. J. Varma and P. Talukdar, *Chem. Commun.*, 2012, **48**, 2722–2724.
10 H. S. Jung, K. C. Ko, G.-H. Kim, A.-R. Lee, Y.-C. Na, C. Kang, J. Y. Lee and J. S. Kim, *Org. Lett.*, 2011, **13**, 1498–1501.
11 Y.-Q. Sun, M. Chen, J. Liu, X. Lv, J. Li and W. Guo, *Chem. Commun.*, 2011, **47**, 11029–11031.
12 H. Wang, G. Zhou, C. Mao and X. Chen, *Dyes Pigm.*, 2013, **96**, 232–236.
13 H. Kwon, K. Lee and H.-J. Kim, *Chem. Commun.*, 2011, **47**, 1773–1775.
14 G.-J. Kim, K. Lee, H. Kwon and H.-J. Kim, *Org. Lett.*, 2011, **13**, 2799–2801.
15 H. S. Jung, J. H. Han, T. Pradhan, S. Kim, S. W. Lee, J. L. Sessler, T. W. Kim, C. Kang and J. S. Kim, *Biomaterials*, 2012, **33**, 945–953.
16 H. S. Jung, T. Pradhan, J. H. Han, K. J. Heo, J. H. Lee, C. Kang and J. S. Kim, *Biomaterials*, 2012, **33**, 8495–8502.
17 X. Chen, S.-K. Ko, M. J. Kim, I. Shin and J. Yoon, *Chem. Commun.*, 2010, **46**, 2751–2753.
18 H.-Y. Shiu, M.-K. Wong and C.-M. Che, *Chem. Commun.*, 2011, **47**, 4367–4369.
19 B. K. McMahon and T. Gunnlaugsson, *J. Am. Chem. Soc.*, 2012, **134**, 10725–10728.
20 M. Hu, J. Fan, H. Li, K. Song, S. Wang, G. Cheng and X. Peng, *Org. Biomol. Chem.*, 2011, **9**, 980–983.
21 X. Liu, N. Xi, S. Liu, Y. Ma, H. Yang, H. Li, J. He, Q. Zhao, F. Li and W. Huang, *J. Mater. Chem.*, 2012, **22**, 7894–7901.
22 P. Wang, J. Liu, X. Lv, Y. Liu, Y. Zhao and W. Guo, *Org. Lett.*, 2012, **14**, 520–523.
23 X. Yang, Y. Guo and R. Strongin, *Angew. Chem., Int. Ed.*, 2011, **50**, 10690–10693.
24 H. Wang, G. Zhou, H. Gai and X. Chen, *Chem. Commun.*, 2012, **48**, 8341–8343.
25 Z. Guo, S. Nam, S. Park and J. Yoon, *Chem. Sci.*, 2012, **3**, 2760–2765.
26 S. Ji, H. Guo, X. Yuan, X. Li, H. Ding, P. Gao, C. Zhao, W. Wu, W. Wu and J. Zhao, *Org. Lett.*, 2011, **12**, 2876–2879.
27 L. Yuan, W. Lin, S. Zhao, W. Gao, B. Chen, L. He and S. Zhu, *J. Am. Chem. Soc.*, 2012, **134**, 13510–13523.

28 X.-D. Jiang, J. Zhang, X. Shaoa and W. Zhao, *Org. Biomol. Chem.*, 2012, **10**, 1966–1968.
29 L.-Y. Niu, Y.-S. Guan, Y.-Z. Chen, L.-Z. Wu, C.-H. Tung and Q.-Z. Yang, *J. Am. Chem. Soc.*, 2012, **134**, 18928–18931.
30 J. H. Lee, C. S. Lim, Y. S. Tian, J. H. Han and B. R. Cho, *J. Am. Chem. Soc.*, 2010, **132**, 1216–1217.
31 C. S. Lim, G. Masanta, H. J. Kim, J. H. Han, H. M. Kim and B. R. Cho, *J. Am. Chem. Soc.*, 2011, **133**, 11132–11135.
32 M. H. Lee, J. H. Han, P.-S. Kwon, S. Bhuniya, J. Y. Kim, J. L. Sessler, C. Kang and J. S. Kim, *J. Am. Chem. Soc.*, 2012, **134**, 1316–1322.
33 B. C. Zhu, X. L. Zhang, Y. M. Li, P. F. Wang, H. Y. Zhang and X. Q. Zhuang, *Chem. Commun.*, 2010, **46**, 5710–5712.
34 C. Ding, H. Li, X. Li and S. Zhang, *Chem. Commun.*, 2010, **46**, 7990–7992.
35 L. Long, W. Lin, B. Chen, W. Gao and L. Yuan, *Chem. Commun.*, 2011, **47**, 893–895.
36 B. Zhu, X. Zhang, H. Jia, Y. Li, S. Chen and S. Zhang, *Dyes Pigm.*, 2010, **86**, 87–92.
37 R. Wang, L. Chen, P. Liu, Q. Zhang and Y. Wang, *Chem.–Eur. J.*, 2012, **18**, 11343–11349.
38 H. S. Jung, J. H. Han, Y. Habata, C. Kang and J. S. Kim, *Chem. Commun.*, 2011, **47**, 5142–5144.
39 H. Wang, G. Zhou and X. Chen, *Sens. Actuators, B*, 2013, **176**, 698–703.
40 Y.-B. Ruan, A.-F. Li, J.-S. Zhao, J.-S. Shen and Y.-B. Jiang, *Chem. Commun.*, 2010, **46**, 4938–4940.
41 Y.-K. Yang, S. Shim and J. Tae, *Chem. Commun.*, 2010, **46**, 7766–7768.
42 N. Y. Kwon, D. Kim, G. Jang, J. H. Lee, J.-H. So, C.-H. Kim, T. H. Kim and T. S. Lee, *ACS Appl. Mater. Interfaces*, 2012, **4**, 1429–1433.
43 Y. Bao, Q. Li, B. Liu, F. Du, J. Tian, H. Wang, Y. Wang and R. Bai, *Chem. Commun.*, 2012, **48**, 118–120.
44 H. Xu, Y. Wang, X. Huang, Y. Li, H. Zhang and X. Zhong, *Analyst*, 2012, **137**, 924–931.
45 L. Zhou, Y. Lin, Z. Huang, J. Ren and X. Qu, *Chem. Commun.*, 2012, **48**, 1147–1149.
46 S.-K. Sun, H.-F. Wang and X.-P. Yan, *Chem. Commun.*, 2011, **47**, 3817–3819.
47 Q. Qian, J. Deng, D. Wang, L. Yang, P. Yu and L. Mao, *Anal. Chem.*, 2012, **84**, 9579–9584.
48 Z. Guan, S. Li, P. B. S. Cheng, N. Zhou, N. Gao and Q.-H. Xu, *ACS Appl. Mater. Interfaces*, 2012, **4**, 5711–5716.
49 F. Pu, Z. Huang, J. Ren and X. Qu, *Anal. Chem.*, 2010, **82**, 8211–8216.
50 W. Y. Xie, W. T. Huang, N. B. Li and H. Q. Luo, *Chem. Commun.*, 2012, **48**, 82–84.